28th Symposium on Naval Hydrodynamics
Pasadena, California, 12-17 September 2010

Numerical Evaluation of Capsizing Probability in Quartering Seas with Split Time Method

Vadim Belenky
(Naval Surface Warfare Center Carderock Division, Maryland, USA)
Kenneth M. Weems, Woei-Min Lin
(Science Applications International Corporation, Bowie, Maryland, USA)
Kostas Spyrou
(National Technical Institute of Athens, Greece)

ABSTRACT

The paper discusses a split-time method to estimate the probability of capsizing of naval ships in irregular quartering seas. The calculation of the probability of capsizing presents a formidable mathematical problem as the roll period and mean time to capsizing are practically incomparable values, which presents the problem of rarity. The split-time method attempts to solve the problem of rarity by separating the solution domain in two or more parts, each of which can be solved separately and efficiently using numerical simulations. The solutions are combined through upcrossing theory and initial conditions, with a careful consideration of the distribution of initial conditions at upcrossing. The use of advanced, physics-based body-nonlinear numerical simulations allows the method to directly evaluate a ship's changing stability as it moves in waves and to consider unconventional as well as conventional hull. The paper also discusses some ideas on how the split-time method can be applied to the probability of capsizing due to broaching, and reviews a study of the ability of potential flow based simulations to predict the phenomena of surf-riding and broaching in regular waves.

INTRODUCTION

Stability failures in stern quartering waves are the result of the interaction of a diverse set of forces and can be realized through several distinct dynamical phenomena. These phenomena include

- Pure loss of stability (attaining a large roll angle or capsizing as the result of decreased stability when the ship is situated around wave crest);
- Parametric roll (dramatic amplification of roll caused by a parametric resonance due to the periodic change of stability in waves);
- Broaching after surf-riding (large roll angle or capsize caused by an uncontrollable violent turn due to directional instability after a ship is caught by a wave and surf-rides on its forward slope);
- Direct broaching (large roll angle or capsizing caused by a sudden amplification of yaw motion resulting from a fold bifurcation in yaw).

The principal forces and effects that drive these dynamical phenomena are quite diverse:

- The hydrostatic, Froude-Krylov, diffraction and radiation forces associated with the large-amplitude wave-body interaction problem drive the change of stability in waves, invoke and damp vertical motions in waves, generate steady and unsteady surging forces that can create a surf-riding equilibrium, and contribute to unsteady sway and yaw motions.
- Vortical (lifting) forces on the hull and appendages are responsible for the primary lateral plane forces and moments that result from unsteady sway and yaw, and can provide a significant coupling between lateral and vertical plane motions, especially roll.
- Viscous effects provide damping in both the vertical and lateral planes, contribute to the surf-riding equilibrium through hull drag, and invoke the vortices associated with lifting forces.
- Propulsion (thrust) forces play its part in creating the surf-riding equilibrium and influence the encounter frequency of waves through forward speed.
- The course keeping autopilot plays a critical role in lateral plane restoring forces and moments including equilibria associated with broaching.
- Anti-rolling systems are very important to roll motion, especially roll motion associated with direct or parametric resonance.

These are the principal forces and effects that need to be considered for the specified dynamical phenomena, but they are not complete. The influence of water on deck or the interaction of deck and water

once the roll angle is large enough, wind forces, and other effects may be important for particular applications, but are neglect here for the simple reason of keeping physical complexity of the problem under control. Even with this reduced list, the complexity of the problem remains formidable as it combines randomness of a realistic seaway with dynamical nonlinearity coming from large-amplitude motions, consideration of which is absolutely necessary for dynamic stability applications.

The realistic modeling of these forces is the key to the realistic modeling of the dynamic phenomena, so advanced hydrodynamic computation codes are necessarily part of solution. However, the necessity of using a statistical description of irregular seas practically rules out high-fidelity CFD tools or model tests as methods for Monte-Carlo simulation due to prohibitive cost of calculations or tests. Potential flow based hydrodynamics with semi-empirical models of viscous and lifting forces remains the only practical option for this type of computational problems. However, model tests or CFD are necessary to provide ship-specific tuning of the semi-empirical models.

Even with relatively fast potential flow hydrodynamic tools, brute-force direct Monte-Carlo simulation remains impractical due to the extreme rarity of stability failures for a ship in a realistic loading condition. On the other hand, the extreme nonlinearity of the stiffness rules out conventional statistical extrapolation methods. The combination of nonlinearity and rarity presents the main challenge to be addressed.

The "separation principle" seems to be an answer to the challenge. Its main idea is to separate rare events from "non-rare" phenomenon that can be handled with statistical method. The solution of the non-rare sub-problem should lead to the probabilistic characteristics of the conditions where the rare event *may* occur. Then conditional probability of whether the rare event actually occurs can be found separately; this is the rare sub-problem.

One good example of the implementation of the separation principle is the wave group approach (Themelis and Spyrou, 2007) where the complex dynamics of a ship is only considered for a relatively short series of large waves. These wave groups are considered as independent random events, while the initial condition at the encounter of a group is evaluated from the relatively mild response between groups. Some of the probabilistic aspects of this approach are examined by Bassler et al. (2010).

Another implementation of the principle of separation is the time-split method originally formulated for a piecewise linear model (Belenky 1993) and developed further by Paroka et al., (2006). The separation here comes in the space of state variables as a roll threshold. The non-rare sub-problem focuses on developing statistics that allow the evaluation of the rate of upcrossing of the threshold. The rare sub-problem finds the probability of a large roll angle or capsizing if the threshold has been crossed, based on the distribution of initial conditions at the instant of crossing. The further development of the method has included the use of an advanced hydrodynamic code for beam seas (Belenky et al. 2008).

In a certain sense, the Peak-over-Threshold (POT) method can be interpreted in terms of the separation principle when applied to dynamic stability (Campbell and Belenky 2010a). Like the time-split method, the non-rare sub-problem is a statistical estimation of upcrossing through the threshold. However, the rare sub-problem is a statistical extrapolation of the peaks exceeding the threshold. The method can be applied to simulation and model test, but is limited by relatively mild nonlinearity; for ship roll, this limit is roughly the angle of maximum of the GZ curve. The method can be used along with an envelope presentation in order to evaluate the probability of stability failure on both sides (Campbell and Belenky 2010b).

This paper is describes the application of split-time method for a ship in stern-quartering seas, focusing on the problem of pure loss of stability and its further development into surf-riding and broaching.

CONCEPT OF THE SPLIT TIME METHOD IN QUARTERING SEAS

In the application of time-split method to capsizing in beam seas (Belenky et al. 2008), the upcrossing threshold was defined as the angle of maximum of the calm-water GZ curve. The most important difference introduced by following and stern quartering seas is changing stability, so the threshold now becomes a stochastic process as well, see Figure 1.

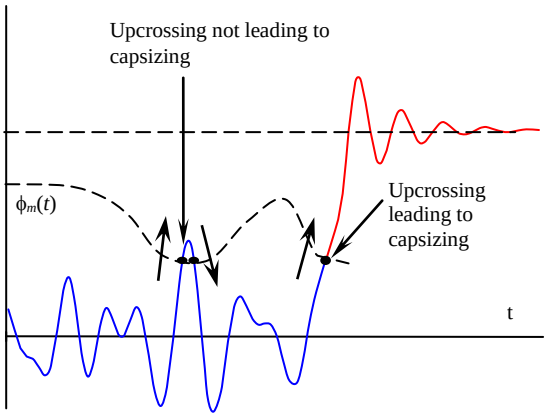

Figure 1: Split-time in quartering seas

The upcrossing problem now needs to consider the time varying threshold as well as the roll motion. It is convenient to introduce a so-called "carrier" process representing an instantaneous

difference between the roll angle at the maximum of the GZ curve and the instantaneous roll angle:

$$x(t) = \phi(t) - \phi_m(t) + \phi_{m0} \qquad (1)$$

Here $\phi(t)$ is current roll angle, $\phi_m(t)$ is the current value of the threshold (instantaneous angle of maximum of GZ curve can be used in certain circumstances), and ϕ_{m0} is the base value for the threshold (maximum of the GZ curve in calm water).

The next step is the calculation of the critical roll rate, which is the minimum roll rate at upcrossing that will lead to capsizing. The procedure for calculating the critical roll rate is illustrated in Figure 2 and consists of a series short simulations starting at the threshold roll angle with different roll rates. An iterative process is used to vary the roll rate by successively finer increments in order to find the boundary between capsize and non-capsize for any given accuracy.

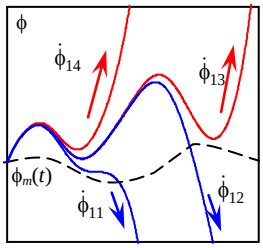

Figure 2: Calculation of critical roll rate

It is important to note that critical roll rate, like the threshold roll angle, is now a stochastic process. As the stiffness of the dynamical system is changing, so does the critical roll rate. The critical roll rate calculation is now repeated for each time value and must consider the change of the roll restoring with time.

This allows the formulation of the complete capsizing conditions: the roll process crosses the threshold and the roll rate at this instant exceeds the critical roll rate calculated for this time. The formulation is identical to that from (Belenky et al. 2008) for beam seas, but the roll threshold and critical roll rate are now stochastic processes in the case of stern quartering waves. This formulation is illustrated in Figure 3 and is expressed in the following formula

$$P_C(T) = 1 - \exp\left(-\xi P_{C|U} T\right) \qquad (2)$$

Here ξ is upcrossing rate of the carrier process (1) or the exceedance rate of the roll angle over the threshold; $P_{C|U}$ is the conditional probability of capsizing if the upcrossing occurs, which is the probability that the roll rate at upcrossing exceeds the critical roll rate:

$$P_{C|U} = P\left(\dot{\phi}(t) > \dot{\phi}_{cr}(t) \,|\, U\right) \qquad (3)$$

Here $\dot{\phi}_{cr}(t)$ is critical roll rate; U is the event of upcrossing of the carrier process (1):

$$U = \left(x(t) = \phi_{m0} \cap \dot{x}(t) > 0\right) = \left(\phi(t) - \phi_m(t) \cap \dot{\phi}(t) > \dot{\phi}_m(t)\right) \qquad (4)$$

The upcrossing rate ξ is than expressed through carrier process and its derivative as

$$\xi = f(x)\int_0^\infty \dot{x} f(\dot{x}) d\dot{x} \qquad (5)$$

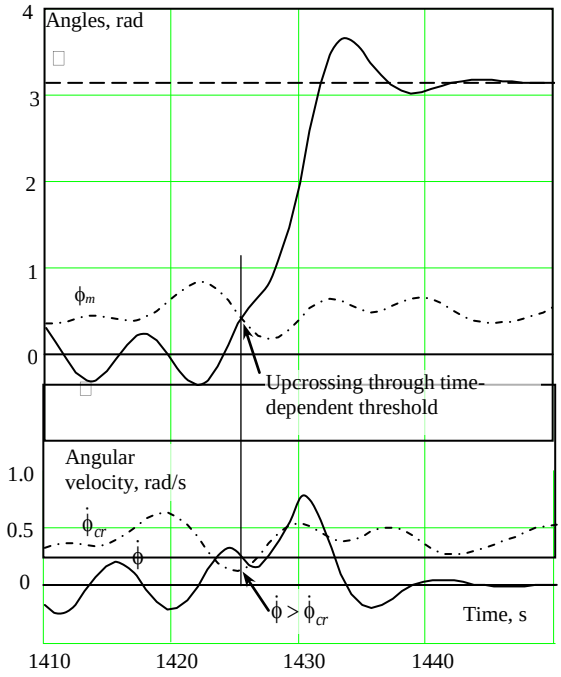

Figure 3: Definition of capsizing with critical roll rate

In the same way that it was convenient to define the carrier process *x(t)*, it makes sense to consider a process of the difference between the instantaneous and critical roll rates, which will be *y(t)*

$$\dot{\phi}_d(t) = \dot{\phi}_{xr}(t) - \dot{\phi}(t) = y(t) \qquad (6)$$

In total, there are three stochastic processes that are needed in order to compute the probability of capsizing in formula (2-5) as illustrated in Figure 3:

- The "carrier" process $x(t)$ defined with formula (1)
- The derivative of the "carrier" process
- The process of the difference between the critical roll rate and the current roll rate $y(t)$ defined with equation (6)

Time histories of all these processes are available from simulation data, and their distribution can be fitted. As the problem is considered in a stationary formulation, the "carrier" and its derivative are independent. However, both the "carrier" and its derivative may be dependent on the difference process $y(t)$. Therefore, the complete probabilistic characterization of these processes requires a three-dimensional joint distribution:

$$f(x, \dot{\phi}_d, \dot{x}) = f(x, y, \dot{x}) \qquad f(x, \dot{x}) = f(x) f(\dot{x}) \qquad (7)$$

As equation (3) is the conditional probability, it requires the distribution of the value of the difference process $y(t)$ at the instant of upcrossing:

$$P_{C|U} = P\left(\dot{\phi}(t) > \dot{\phi}_{cr}(t) \,|\, U\right) = P\left(y(t) < 0 \,|\, U\right)$$
$$= P\left(y(t_c) < 0\right) = \int_{-\infty}^{0} f_c(y_c)\,dy_c \qquad (8)$$

Here index "c" refers to values taken at the moment of crossing: y_c is the value of the difference process $y(t)$ taken at the instant of crossing t_c while f_c is its PDF.

To solve the rare sub-problem, this PDF needs to be found. The problem can be formulated in general terms: there are two stationary processes x(t) and $y(t)$. They are dependent. At the time instant t_c the process x upcrosses a given threshold. It is necessary to find the distribution of the value of the process y at this instant, see Figure 4.

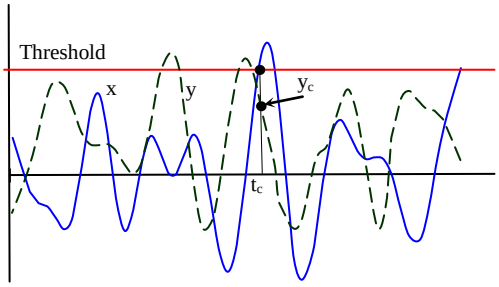

Figure 4: Value of dependent process at upcrossing

DISTRIBUTIONS AT UPCROSSING

The problem of the distribution of the value of one process at an instant of upcrossing of a second process was first encountered by one of the authors in relation with the application of the piecewise linear method for the calculation of the probability of capsizing in beam seas (Belenky 1993). That method required a value of roll rate when the roll angle crosses the level of maximum of the GZ curve. For the case of a piecewise linear system, the process of roll angles is normal. As the roll rates are independent from roll, an argument was made that any positive value of roll rate can be encountered at the upcrossing of roll. Therefore, a truncated normal distribution was used for the roll rates at upcrossing.

However, while carrying out a self-consistency check of the time-split method using the piecewise linear system, it was found that the roll rate at upcrossing follows a Rayleigh distribution (Belenky et al., 2008). The key is that the distribution of the derivative would remain the same if sampling was random, but sampling at the instant of the upcrossing of the process is *not* random. Further investigation showed that the distribution of the derivative of a process at upcrossing can be expressed through the following formula:

$$f_c(\dot{x}_c) = \frac{\dot{x}_c f(\dot{x}_c)}{\int_0^{\infty} \dot{x} f(\dot{x})\,d\dot{x}} \qquad (9)$$

Expression (9) becomes a Rayleigh distribution for a normally distributed derivative, which is consistent with the observation for the piecewise linear system. A brief derivation of (9) is presented in Appendix 1 of this paper, while details can be found in Appendix 3 of the final version of Belenky, et al., (2008).

The problem with the distribution of the value of a dependent process at upcrossing is quite similar in nature. Following a similar derivation, the distribution of the dependent process $y(t)$ while the process $x(t)$ upcrosses a threshold a can be expressed as:

$$f_c(y_c) = \frac{\int_0^{\infty} \dot{x} f(a, \dot{x}, y_c)\,d\dot{x}}{f(a)\int_0^{\infty} \dot{x} f(\dot{x})\,d\dot{x}} \qquad (10)$$

As above, the index "c" refers to values taken at the moment of crossing. A brief version of the derivation is included as Appendix 2 of this paper while details can be found in Belenky et al. (2009).

In order to check these derivations, a series of statistical tests were carried out. Wave elevations for a linear irregular sea corresponding to Sea State 8 ($H^{1/3}$=11.49m, T_0=16.4s) were used as the process for upcrossings:

$$\zeta_W(t) = \sum_i r_i \cos\left(\omega_i t + \varphi_i\right) \qquad (11)$$

Here r_i specifies a set of component wave amplitude calculated with Bretschneider spectrum with frequency set ω_i and random phase φ_i following a uniform distribution from 0 to 2π. The dependent process $\psi(t)$ is created by applying a phase shift:

$$\psi(t) = \sum_i r_i \cos\left(\omega_i t + \varphi_i + \varepsilon(\omega_i)\right) \qquad (12)$$

Where the phase shift is defined as:

$$\varepsilon(\omega) = \arctan\left(\frac{2\omega\delta_p}{\omega^2 - \delta_p^2}\right) \qquad (13)$$

Here δ_p is a phase shift parameter δ_p = 0.5. The derivative of the wave elevation is:

$$\dot{\zeta}_W(t) = -\sum_i r_i \omega_i \sin\left(\omega_i t + \varphi_i\right) \qquad (14)$$

As all three processes are normal, their dependence is completely expressed through correlation coefficients:

$$k_{\zeta\psi} = 0.29 \quad k_{\dot{\zeta}\psi} = 0.68 \quad k_{\zeta\dot{\zeta}} = 0 \qquad (15)$$

1000 records, each of 30 minutes duration, were generated for the test. The threshold value was set to 9 m and 688 upcrossings were observed. The distribution of the derivative at upcrossing is shown in Figure 5, while the distribution of the value of dependent process ψ_c is shown in Figure 6. Chi-square goodness of fit test does not reject either formulae (9) or (10).

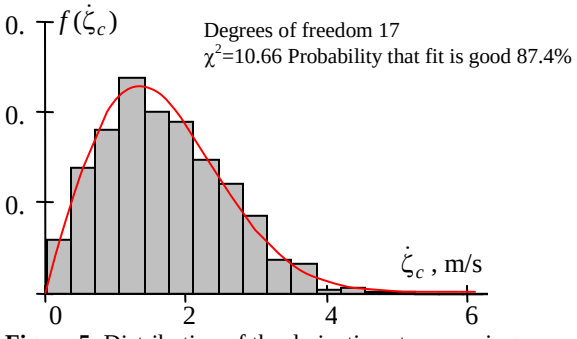

Figure 5: Distribution of the derivative at upcrossing

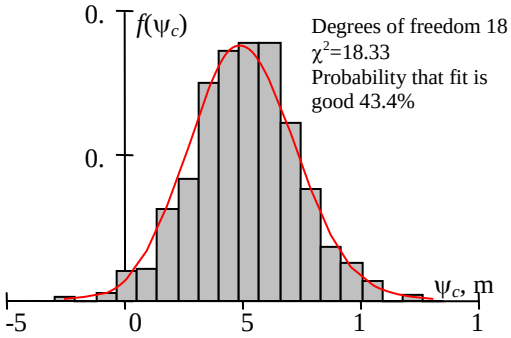

Figure 6: Distribution of the dependent process at upcrossing

TEST OF THE CONCEPT

In order to test the formulation of the time-split concept with changing stability in waves, a piecewise linear dynamical system with random elements of stiffness was used (Belenky et al. 2009). A brief description of the solution is presented blow; details can be found in the above reference. In order to retain a closed-form solution, only the decreasing part of stiffness curve is allowed to change, see Figures 7 and 8.

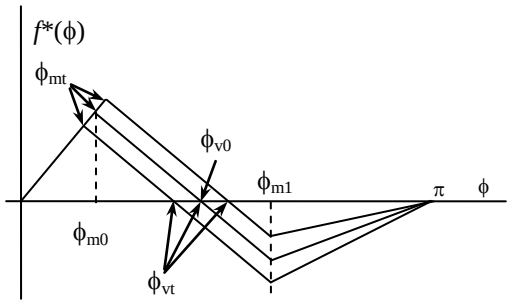

Figure 7: Piecewise linear stiffness term with time-varying decreasing part

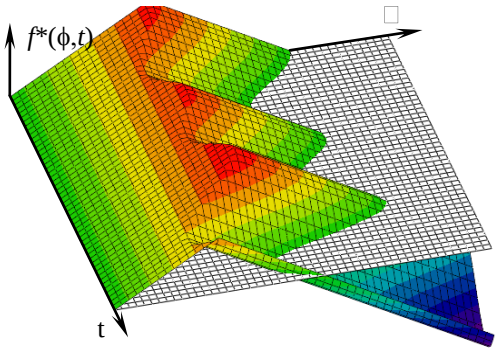

Figure 8: Piecewise linear stiffness term with time-varying decreasing part as a surface

The maximum of the GZ curve is assumed to be a linear function of heave motions:

$$\phi_m(t) = \frac{\phi_{m0}}{\omega_0^2}\left(k_d\left(\zeta(t)+d\right)+b_d\right) \qquad (16)$$

Here k_d, b_d and d are stiffness parameters and ω_0 is the roll natural frequency. The heave motion is defined by the linear differential equation:

$$\ddot{\zeta} + 2\delta_\zeta\dot{\zeta} + \omega_\zeta^2\zeta = f_{E\zeta}(t)\,. \qquad (17)$$

Where $f_{E\zeta}$ is wave excitation, δ_ζ is a notional heave damping, and ω_ζ is the natural frequency of heave. Formulae (16) and (17) allow the time history of the angle of the maximum of the GZ curve to be expressed in the form of a Fourier series:

$$\phi_m(t) = \phi_{m0} + \sum_{i=1}^{N_\omega}\phi_{mai}\cos(\omega_i t + \gamma_{\zeta i} + \varphi_i) \quad (18)$$

Formulae for the amplitude ϕ_{mai} and phase γ_ζ. can be found in Belenky et al. (2009).

Roll is defined with the following differential equation with piecewise linear stiffness:

$$\ddot{\phi} + 2\delta_\phi\dot{\phi} + f^*(\phi) = f_{E\phi}(t). \qquad (19)$$

Where $f_{E\phi}$ is wave excitation and δ_ϕ is a roll damping coefficient. The piecewise linear stiffness is expressed as:

$$f^*(\phi) = \omega_0^2\begin{cases}\phi & |\phi| < \phi_m(t)\\ k_1\phi + b_1(t) & |\phi| \geq \phi_m(t)\,,\end{cases} \qquad (20)$$

Where k_1 is a contact coefficient, while $b_1(t)$ is a stochastic process which is a deterministic function of random angle of maximum $\phi_m(t)$.

The solution of equation (19) between the cases of exceedance of the angle of maximum (they are assumed to be rare) can be expressed as Fourier series, as can the time history of the carrier process (1):

$$x(t) = \phi_{m0} + \sum_{i=1}^{N_\omega}x_{ai}\cos(\omega_i t + \gamma_{xi} + \varphi_i) \qquad (21)$$

Where x_{ai} is a component amplitude and γ_{xi} is the phase.

The solution of the non-rare sub-problem is trivial as the carrier process is normal, so the rate of upcrossing is expressed as:

$$\xi = \sqrt{\frac{V_{\dot{x}}}{V_x}} \exp\left(-\frac{\phi_{m0}^2}{2V_x}\right) \qquad (22)$$

Where the variance of the carrier, V_x, and its derivative, $V_{\dot{x}}$, are trivially derived from their Fourier presentations.

The objective of the rare sub-problem is to find the critical roll rate and its probabilistic characteristics. The roll equation remains linear after upcrossing:

$$\ddot{\phi} + 2\delta\dot{\phi} + k_1\phi = k_b\zeta(t) + k_1\phi_{v0} \qquad (23)$$

Here ϕ_{v0} is angle vanishing stability – the position of unstable equilibrium in calm water and $k_b = k_1 k_d$. Its total solution consists of the general solution of the homogeneous equation and a particular solution of the original heterogeneous equation:

$$\phi(t) = \phi_H(t) + p(t) \qquad (24)$$

The solution of the homogeneous equation is

$$\phi_H(t) = A\exp(\lambda_1 t) + B\exp(\lambda_2 t) \qquad (25)$$

Here $\lambda_{1,2}$ are eigenvalues and A and B are arbitrary constants. One of eigenvalues λ_1 is positive, so the sign of the arbitrary constant A determines whether capsize will occur after this upcrossing.

$$A = \frac{(\dot{\phi}(t_c) - \dot{p}(t_c)) - \lambda_2\left(\phi_m(t_c) - \phi_{v0} - p(t_c)\right)}{\lambda_1 - \lambda_2} \qquad (26)$$

$p(t_c)$ and $\dot{p}(t_c)$ are the values of the particular solution at the instant of upcrossing t_c.

The critical roll rate is the value of the initial roll rate $\dot{\phi}(t_c)$ in formula (26) that turns the arbitrary constant to zero; therefore:

$$\dot{\phi}_{cr}(t) = \lambda_2\left(\phi_m(t) - \phi_{v0} - p(t)\right) + \dot{p}(t) \qquad (27)$$

This allows the difference between the critical roll rate and the current roll rate to be expressed through the Fourier series:

$$\dot{\phi}_d(t) = \lambda_2(\phi_{m0} - \phi_{v0}) + \sum_{i=1}^{N_\omega} a_{rdi}\cos(\omega_i t + \gamma_{rdi} + \varphi_i) = y(t) \qquad (28)$$

All three of the processes required for the split-time concept in quartering seas are now presented in the form of Fourier series. All are normal and the dependence between these processes is completely described by correlation, which can be trivially calculated from Fourier series presentation. Substitution of the three-dimensional normal distribution into formula (10) yields the following expression for the distribution of the difference between the critical and current roll rates at upcrossing:

$$f_c(\dot{\phi}_d) = \frac{\sqrt{2\pi}}{\sigma_{\dot{x}}}\int_0^\infty \dot{x} f(x = \phi_{m0}, \dot{x}, \dot{\phi}_d) d\dot{x} \qquad (29)$$

This expression can be plugged into formula (8) to get the probability of capsizing after upcrossing.

In order to verify the self-consistency of these results, a series of Monte-Carlo simulations were performed for the notional ship with piecewise linear stiffness in Sea State 8. In the first series of 200 records of 30 minutes each, 70 records end up capsizing. Figure 9 compares the theoretical and statistical solutions of rare sub-problem. The two solutions show good agreement in both the distribution of the difference between critical and current roll rate and the probability of capsizing after upcrossing.

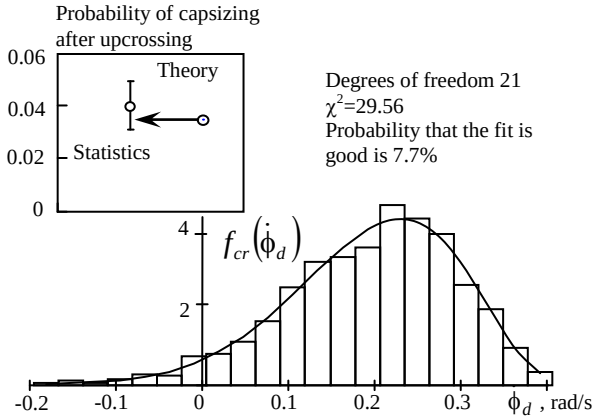

Figure 9: Distribution of the distance between critical and instantaneous roll rate at upcrossing.

In order to see if the statistical estimate of the probability of capsizing converges to the theoretical solution (2), two convergence checks were performed with independent sets of initial phases. Each check consisted of estimating the probability of capsizing on an increasing number of 30-minute records from 200 to 6000. Figure 10 plots the statistical probability of capsize with confidence interval versus the theoretical value predicted with the time-split method. The statistical results do not reject the theory and show a clear tendency to converge to the result of formula (2). Details of the calculation can be found in Belenky et al. (2009).

LAMP IMPLEMENTATION

While the concept of the time-split method has largely been developed using an ordinary differential equation for roll with piecewise linear stiffness, the goal is to implement the time-split method using numerical simulations from advanced time-domain numerical seakeeping codes. In the present work, the method is being implemented with the LAMP (Large Amplitude Motions Program) code.

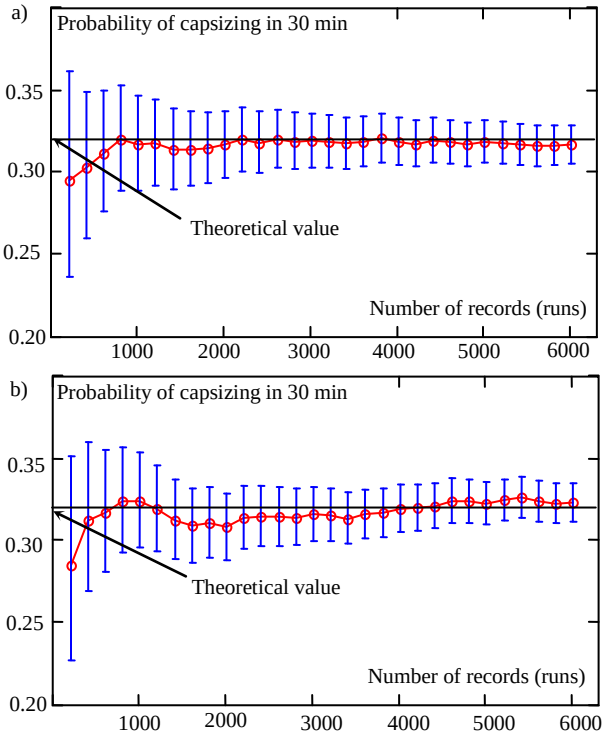

Figure 11 Convergence of the statistical frequency to theoretical solution as number of runs increases. Upper (a) and lower (b) graphs differ in sets of initial phases

LAMP is a nonlinear time-domain potential flow seakeeping code developed to predict the motions and loads of a ship or other marine vehicle in a seaway. The core of the LAMP calculation is the solution of the wave-body interaction problem in the time domain using a 3-D potential flow panel method. The hydrodynamic forces are integrated with a variety of models for additional effects and systems, including viscous and lifting forces for hull and appendages, as well as course and motion control systems to provide a comprehensive model of a ship operating in a seaway. A key element of the LAMP calculation is the 3-D body-nonlinear calculation of the incident wave (Froude-Krylov) and hydrostatic restoring forces. These forces are computed by integrating the Froude-Krylov and hydrostatic pressure of the instantaneous wetted portion of the hull at its predicted position and beneath the incident wave at each time step. The body-nonlinear hydrostatics has been found to be the dominating effect in both nonlinear ship wave loads in extreme seas (Weems et al. 1998) and the parametric roll of container carriers, and is critical for evaluating the roll restoring of unconventional hull forms and the variation of roll restoring in waves (Belenky and Weems 2008).

EVALUATION OF THE GZ CURVE IN WAVES

In order to apply the time-split method for quartering seas with a hydrodynamic code, it is necessary to evaluate the ship's instantaneous roll restoring (GZ) curve as it moves in waves. In principle, this evaluation is not much different from evaluating the calm water GZ curve in the model tank: the ship is rolled through a series of incremental heel angles and the restoring moment and GZ are calculated for each heel angle. The differences are that the GZ curve is computed at each time step of the simulation and the heel angles are applied as a variation to the predicted instantaneous position on the wave.

Per d'Alembert, any dynamic problem can be considered as a static one if inertia forces and moments are included, so the instantaneous position of a ship in waves can be treated as equilibrium. When the ship is heeled relative to this position, this equilibrium is disturbed as the submerged part of the hull changes, and the forces on the hull change. If the ship is "balanced" on the wave in order to maintain the equilibrium in the heave and pitch, then the resulting moment in roll represents the "pure" heeling moment needed to achieve the incremental heeling angle, and can be directly used to construct an effective GZ curve in waves. The approach is similar to the "wave pass" evaluation of the GZ curve implemented in some static stability programs, but differs in that it considers the equilibrium of the predicted ship motion in the d'Alembert sense (with inertia forces and moments included) rather than a quasi-static equilibrium based on the ship mass and center of gravity.

This calculation of the instantaneous GZ curve in waves has been implemented in the LAMP (Large Amplitude Motions Program) code as part of its time domain ship motions simulation. The procedure is fairly straightforward:

- For each time step of the calculation, the ship is heeled through a range of angles relative to its predicted position
- At each heel angle, the forces and moments on the ship are computed for the heeled position
- The ship's heave position and pitch angle, as expressed relative to a global system, are iteratively adjusted until the dynamic equilibrium in these modes is achieved
- The net roll moment defines an instantaneous GZ value

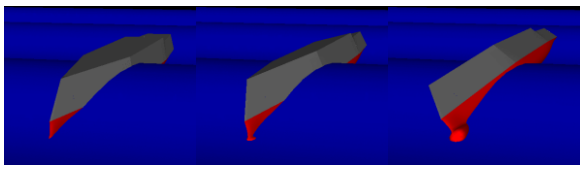

Figure 12 Applying an incremental heeling angle on the ONR Topsides tumblehome hull form in the calculation of the GZ curve in waves

Figure 12 shows how the incremental heeling angle is applied to the ship relative to its instantaneous position on the wave. The ship in this case is the tumblehome variant of the ONR Topsides hull form

series. Figure 13 shows a set of GZ curves for this ship at different times as it runs in regular quartering seas.

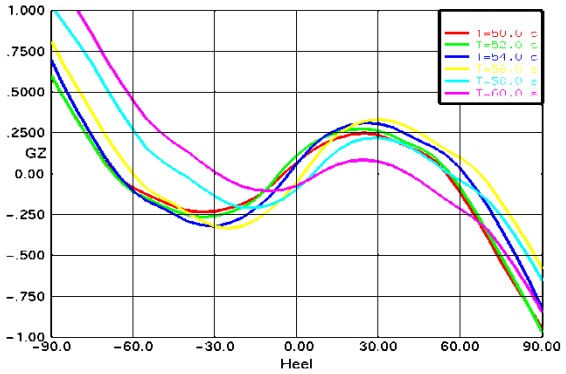

Figure 13 Applying an incremental heeling angle on the ONR Topsides tumblehome hull form in the calculation of the GZ curve in waves

In the calculation of the forces moments on the ship at each heel angle, it is assumed that the inertial forces remain constant – this is the equilibrium in the d'Alembert sense that is maintained. The variation in the hydrostatic and the incident wave forcing is computed by integrating the static and Froude-Krylov pressure over the wetted hull surface at this position. It is assumed that the hydrodynamic forces associated with radiation and diffraction, remain constant. While the effect of the heel angle on these forces is felt to be small compared the hydrostatics and Froude-Krylov forces, this is somewhat of an approximation. However, the hysteresis of the wave-body disturbance problem – the fact that the disturbance is dependent on how the ship got to its position on the wave – makes it impractical to consider the roll variation in the calculation of these forces. The change in the forces and moments due to other effects such as rudder, bilge-keels and anti-rolling systems can be included to some extent, but are typically not significant.

Additional details on the method of calculation, its verification and statistical characteristics of the elements of the GZ curve in waves can be found in Belenky and Weems (2008).

EVALUATION OF THE THRESHOLD

Once the GZ curve has been calculated, it is necessary to determine the upcrossing threshold angles – one positive (rolling to starboard) and one negative (rolling to port) – which are needed to calculate the carrier process *x(t)* as defined in formula (1). Following the general derivation of the time-split problem, this should be the location of the maximum value of the GZ curve. However, the shape of the GZ curve can vary dramatically for a ship moving in large waves, and can have times for which it has multiple local maxima or no positive restoring at all, as illustrated in Figure 14. This makes the maximum point impractical for this application.

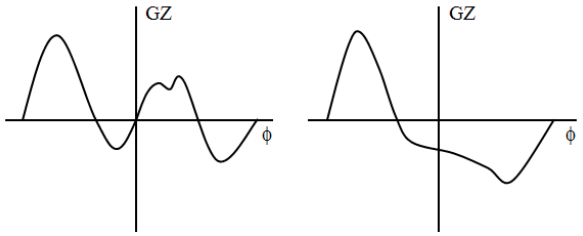

Figure 14 GZ curves in waves showing multiple local maxima and no maximum on positive side

In order to implement the split time method in a hydrodynamic code like LAMP, it is necessary to find a threshold roll angle with the following features:

It is continuous and differentiable.

It is representative of the maximum restoring arm.

There is no significant increase in the restoring arm beyond the threshold value.

The last of these features is necessary in order to preserve an important aspect of the split time method's separation of the roll problem; namely that resonant wave induced motion does not play a significant role in the solution of the rare problem.

For time steps with any positive stability on the given side, including the fairly normal GZ curves shown in Figure 13 and "double hump" example on the left hand side of Figure 14, a suitable threshold angle can be found by calculating the centroid of the top portion of the area under the GZ curve, as illustrated by the schematic in Figure 15. This top area is identified by computing a cut-off level which is set so that the area above the plane and below the GZ curve is equal to:

$$GZ_{Cut} = 0.3 \cdot \phi_V \cdot \max\left(GZ_{\max}, GZ(0)\right) \quad (30)$$

Where ϕ_V is the angle of vanishing stability and $GZ_{\max}$ is the maximum of the *GZ* curve, while GZ(0) is the value of the *GZ* curve for zero roll angle.

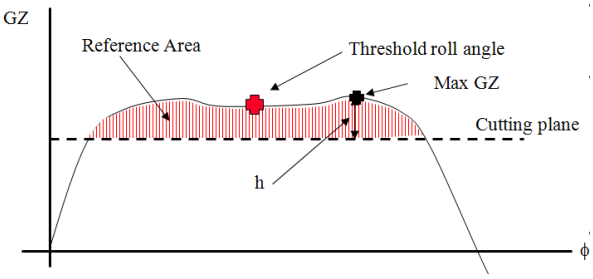

Figure 15 Calculation of the threshold roll angle as the centroid of the area under the top of the GZ curve

This use of the cut-off plane and area centroid has been found to give very stable, reliable, and differentiable values of the threshold roll angle for many lengthy simulations of the tumblehome hull form in large quartering waves.

Figure 15 show a section of time history of the "raw" GZ curve maximum and the threshold value

computed by the area centroid method. The high frequency oscillations in the raw maximum occur when the top of the GZ curve is very flat. The sudden drops occur in a multi-hump curve as the humps change relative size. In both cases, the new scheme produces a stable, reliable value. The scheme can even be used for cases where the peak is below the axis.

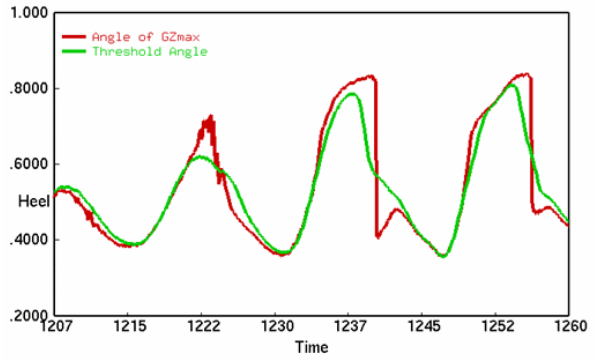

Figure 16 Position of maximum of GZ curve and threshold role angle for tumblehome hull at 15 knots in quartering Sea State 7

For time steps with no positive stability or negative peak on a given side, such as the right hand side example in Figure 14, the threshold value is simply interpolated in time between the last and next time step for which suitable values could be calculated. While this is a somewhat degenerate solution, it satisfies all of the requirements for the threshold value and has worked well for the tumblehome cases.

NON-RARE PROBLEM

In Belenky et al. (2008), the non-rare problem for beam seas was solved by estimating the variance of the roll angles and rates, fitting distributions to the data, and calculating the upcrossing rate as:

$$\xi = f(\phi_{m0}) \int_0^\infty \dot{\phi} f(\dot{\phi}) d\dot{\phi} \qquad (31)$$

However, when this technique was applied to the results of a set of LAMP simulation for the ONR tumblehome hull in stern quartering seas (200 records, 40 min each, sea state 7, speed 15 knots, heading 45 degrees), the number of observed upcrossings was significantly less than expected.

A special study was performed in order to find the reason of this discrepancy. The upcrossing rate through a constant threshold was estimated and compared with the prediction (31) using fitted distributions of roll angles and rates. The comparison has shown a significant difference between the estimate and prediction, as shown in Figure 17.

The formula (31) uses the assumption of the stationarity of the process that results in the independence of the process and its first derivative. Without this assumption, the upcrossing rate can is expressed in terms of a joint distribution as:

$$\xi = \int_0^\infty \dot{\phi} f(\phi_{m0}, \dot{\phi}) d\dot{\phi} \qquad (32)$$

When a joint distribution was fitted for the roll angles and rates, formula (32) yielded a result that falls within confidence interval of statistical estimate of upcrossing rate, as shown in Figure 17.

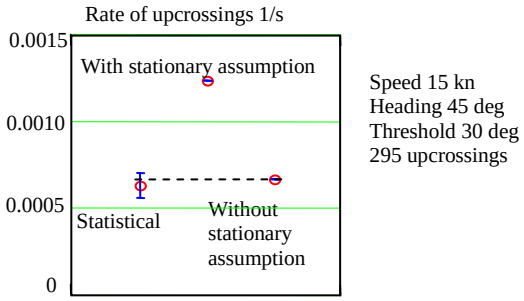

Figure 17 Observed and predicted rate of upcrossing: speed 15 kn

The result at Figure 17 may look like the roll process is not stationary, but there is no physical reason for non-stationarity as stationary waves were the only external excitation and nothing changes within the system. Therefore, the observed effect cannot be a result of real non-stationarity. To see how stable the observed effect is, the calculations were repeated for a heading of 40 degrees and speed of 14 knots (Figure 18).

The results in Figure 18 are very similar to those one in Figure 17; the observed effect seems to be robust. The effect was not observed when the calculations were repeated for zero speed and beam seas, as shown Figure 19. This indicates that the effect is caused by speed and heading.

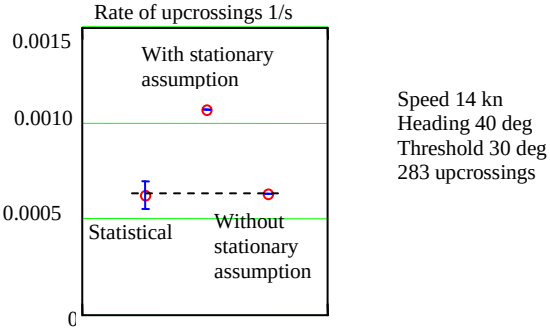

Figure 18 Observed and predicted rate of upcrossings: speed 14 knots, 40° heading

The spectrum of the roll response for the 15 knots case is shown in Figure 20. The curve has a clear "bump" in the area of lower frequencies that can be attributed to Doppler effect. In contrast, the spectrum for the beam seas (Figure 21) has only one peak.

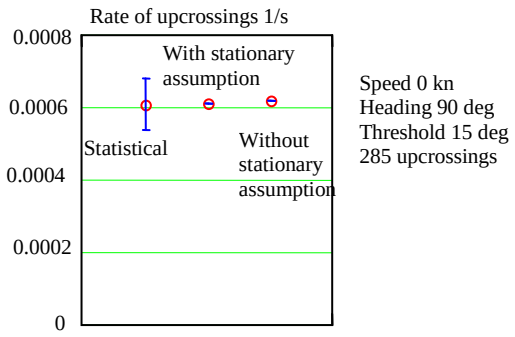

Figure 19 Observed and predicted rate of upcrossings: zero speed, beam seas

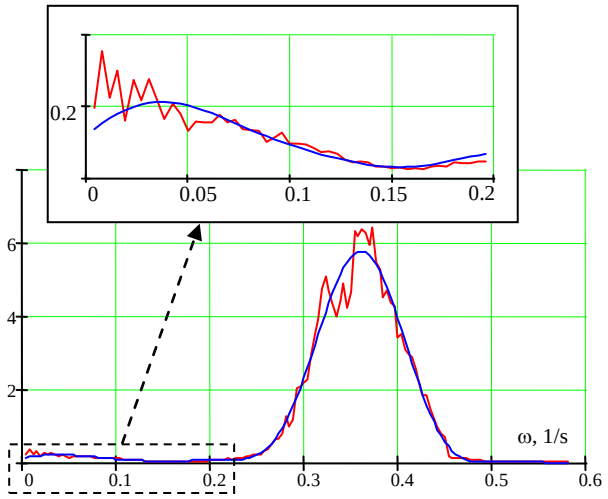

Figure 20 Spectrum of roll response for 15 kn case (red – averaged spectrum, blue averaged and smoothed spectrum)

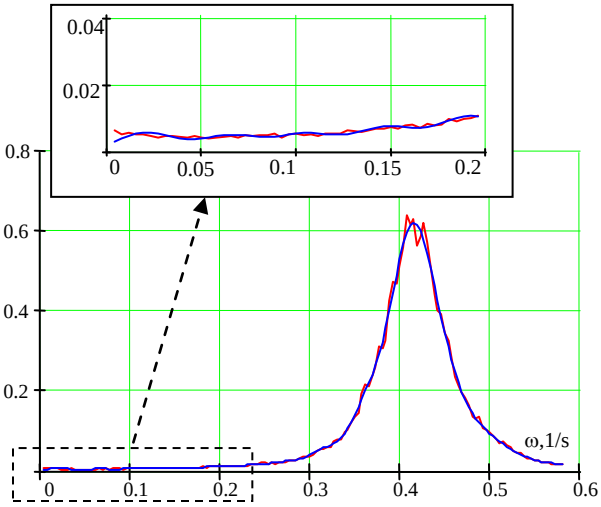

Figure 21 Spectrum of roll response for zero-speed case. (red – averaged spectrum, blue averaged and smoothed spectrum)

The appearance of low-frequency response components in following and stern quartering seas is a well-known effect, and is associated with low encounter frequency. It is also clear that low frequency components may look like non-stationarity; as very long records are required to describe low-frequency components properly. What is surprising is how large this effect was for the upcrossing rate, considering how small the second peak of spectrum is in Figure 20.

It is not clear at this time why this influence is so large and what (if any) influence the changing stability in waves may have towards this effect. It is clear, however, that the effect is strong enough that it must be accounted for in the procedure. The use extrapolation with peak-over-threshold method for estimates of the upcrossing rate may be an option, as proposed by Campbell and Belenky (2010a).

RARE PROBLEM

The objective of the rare problem is the calculation of the probability of capsizing after the threshold has been crossed. This random event is associated with the exceedance of a critical value by current roll rate at the instant of upcrossing, which corresponds to a negative value for the difference process $y(t)$ defined by formula (6). The probability of this event is described by formula (8); while the distribution of the difference process $y(t)$ at upcrossing is determined by (10). The most challenging part is the evaluation of the joint distribution of three processes: the carrier, its derivative and the difference process.

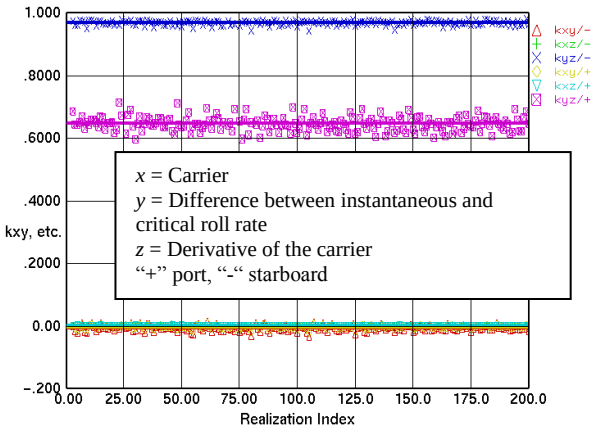

Figure 22 Correlation coefficients for 200 realizations speed 15 knots, heading 45 degrees.

Among these three processes, two are independent due to stationarity: carrier and its derivative (provided that the records are long enough for low-frequency components). All other processes, in principle, need to be treated as dependent. Figure 22 shows correlation coefficients calculated for each realization of simulations for of 15 knots, 45° heading. The ensemble estimate was calculated as an average over all realizations. Calculations were carried out for roll to both sides.

These calculations have shown that significant correlation exists only between the derivative of the carrier and the difference process $y(t)$. It therefore make sense to assume independence of the carrier process $x(t)$ and the process of difference $y(t)$. This allows the problem to be significantly simplified as the

joint distribution of the three processes in formula (10) can be presented as

$$f(x,\dot{x},\dot{\phi}_d) = f(x)\,f(\dot{x},\dot{\phi}_d) \qquad (33)$$

Substitution of (33) in (10) leads to:

$$f_c(\dot{\phi}_d) = \frac{\int_0^\infty \dot{x} f(\dot{x},\dot{\phi}_d)\,d\dot{x}}{\int_0^\infty \dot{x} f(\dot{x})\,d\dot{x}} \qquad (34)$$

As a result the. distribution of the difference process at upcrossing becomes independent on the threshold.

To use formula (34), the joint distribution of the difference process $\dot{\phi}_d(t) = y(t)$ and the derivative of the carrier $\dot{x}(t)$ needs to be fitted. To fit this joint distribution, it is presented as:

$$f(\dot{x},\dot{\phi}_d) = f(\dot{\phi}_d)\,f(\dot{x}\,|\,\dot{\phi}_d) \qquad (35)$$

A Pierson type IV distribution was used to present the conditional distribution of the derivative of the carrier when the difference between instantaneous and critical roll rates took a certain value:

$$f(\dot{x}\,|\,\dot{\phi}_d) = k\left[1+\left(\frac{\dot{x}-\lambda(\dot{\phi}_d))}{a}\right)^2\right]^m \cdot \exp\left[-\nu\tan^{-1}\left(\frac{\dot{x}-\lambda(\dot{\phi}_d))}{a}\right)\right] \qquad (36)$$

The parameters of this Pierson type IV distribution were calculated using the method of maximum likelihood. The parameter λ was considered to be a function of difference process; others did not show significant variability. A Gram-Charlier distribution was used for the marginal distribution of the difference process:

$$f(\dot{\phi}_d) = \frac{1}{\sigma_d\cdot\sqrt{2\pi}}\exp\left(-\frac{u^2}{2}\right)\cdot \left(1-\frac{Sk}{3!}(3u-u^3)+\frac{Ex}{4!}(u^4-6u^2+3)\right) \qquad (37)$$

$$u = \frac{\dot{\phi}_d - m_d}{\sigma_d}$$

Here σ_d and m_d are the standard deviation and mean value of the difference process that are estimated from statistics, while *Sk* and *Ex* are skewness and excess kurtosis that are evaluated with the maximum likelihood method. The result is a fitted joint distribution as shown in Figure 23.

The next step is to fit the marginal distribution of the derivative of the carrier (Gram-Charlier distribution is used) and then apply formula (34). The resulting distribution of the value of the difference process at the upcrossing is shown in Figure 24.

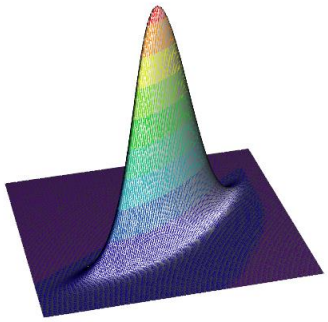

Figure 23 Fitted joint distribution of the difference process and the derivative of the carrier

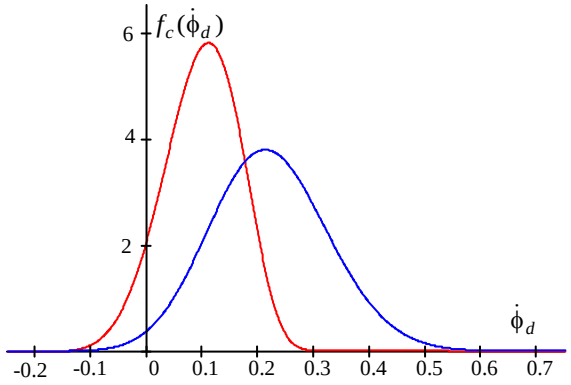

Figure 24 Distributions of the difference process and its value at the instant of the upcrossing of the carrier

The last step is the application of formula (8). This procedure, however, may be vulnerable to a type of numeric error, similar to the one found for non-rare problem. Similar to the non-rare problem, statistical extrapolation may be considered as an alternative, which is an item for future work.

NUMERICAL MODELING OF BROACHING AND SURF-RIDING

Stability failure due to broaching involves a violent uncontrollable turn in waves that could be result of either a directional instability of the surf-riding equilibria or a fold bifurcation of yaw motion. Both these mechanism of broaching are related with maneuvering in waves. The key lateral plane maneuvering forces on the hull and a rudder are vertical or viscous in nature and cannot be modeled natively within a potential hydrodynamic code like LAMP, so supplemental maneuvering force models are required. The implementation of such models must be done carefully in order to avoid double counting with wave-body hydrodynamics and seakeeping force models, and to maintain the applicability of such models, which are typically develop from 3 or 4-DOF tests in calm water, to 6-DOF simulations in waves. The LAMP system has implemented a set of component (*e.g.* rudder, propeller) models plus

standard maneuvering force-derivative models that can be tuned to data from captive model test or high-fidelity CFD simulations. The use of these tuned force models has resulted in good predictions of ship maneuvering in both calm water and waves (Yen, et al. 2010).

In addition the validation of maneuvering in waves, studies have been to verify LAMP's ability to predict the principle dynamic phenomena associated with broaching and capsizing due to broaching; some of these are reviewed below. First, it is ability to reproduce large heel angle (up to capsize) caused by a sharp turn. Figure 25 shows LAMP-predicted time histories of roll for the ONR tumblehome hull with two GM values after a 30° rudder application while sailing 38 knots in calm water. At the higher GM value, the ship attains a large heel angle before recovering. At the lower value, it capsizes.

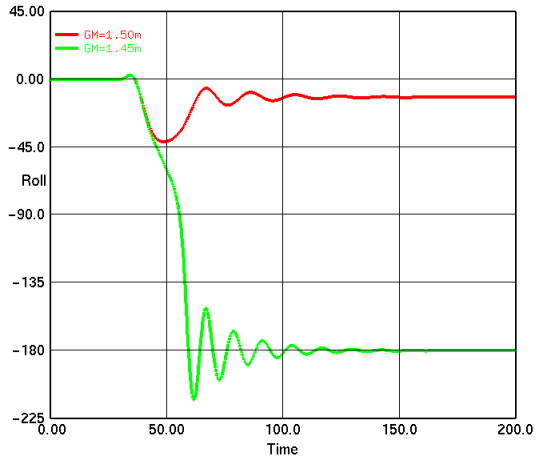

Figure 25 Large heel angle and capsizing due to sharp turn in calm water

Surf-riding is a dynamical equilibrium created (at least) by thrust, resistance and wave forces. It comes into existence when the speed is high enough and the wave is large enough that wave forces are able to accelerate the ship to wave celerity. The whole picture is shown in Figure 26.

As can be seen from Figure 26, there is only surging when the nominal Froude number is below the first critical value Fn_{cr1}. Once this value is exceeded, wave forces added to thrust can accelerate a ship up to the wave celerity. At this range of speeds, surf-riding and unsteady surging co-exist, and can result from different sets of initial conditions. Once the second critical value of nominal Froude number Fn_{cr1} is exceeded, surging seizes to exist and surf-riding remains the only option (Spyrou 1996).

Spyrou et al. (2009) studied patterns of behavior of ONR Topsides series tumblehome hull using LAMP. Figure 27 shows time histories from one of the cases when surging and surf-riding co-exist and the type of the response should depend only on initial conditions. The results of LAMP simulations reproduced this expected behavior precisely.

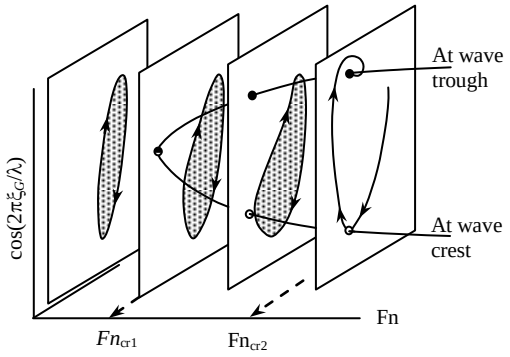

Figure 26 Surging and surf-riding

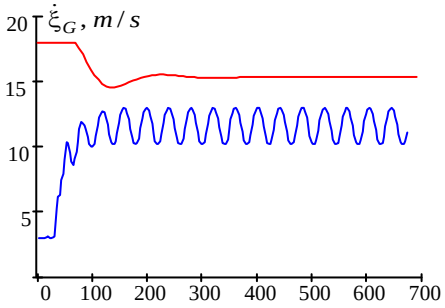

Figure 27 LAMP modeling of coexistence of surging and surf-riding.

Another dynamical mechanism of broaching is related to a fold bifurcation in yaw motions (Spyrou 1997). This phenomenon strongly depends on control setting and can be observed as a sudden amplification of yaw motions. Figure 28 shows a theoretical yaw response curve, where the requested course angle ψ_r is used as a control parameter. There is a range of the requested course angle where three yaw responses exist: two stable and one unstable between them. The theory also predicts that the yaw responses will be subharmonic for some values of the course angle.

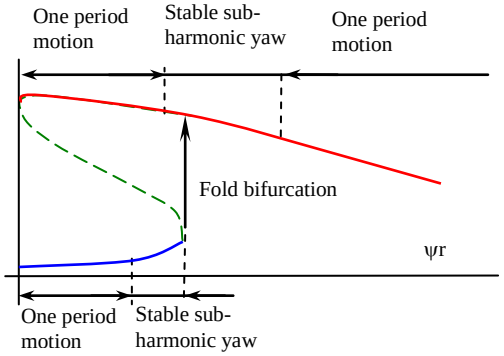

Figure 28 Fold bifurcation in yaw motions

Figure 29 shows yaw motion time histories from three LAMP simulations for the same wave conditions with different requested course angles. All three time histories show subharmonic yaw. Figure 29a shows large-amplitude stable subharmonic yaw for a course angle of 14°, while Figure 29c shows small-amplitude stable sub-harmonic yaw for course of 10°. The response for an intermediate value for the course angle (12°) is shown in Figure 29b. The yaw motion

starts with small amplitude and then "jumps" to the large-amplitude mode. This is a typical picture of fold bifurcation, demonstrating the ability of advance potential codes to model this type of nonlinear behavior in the lateral plane.

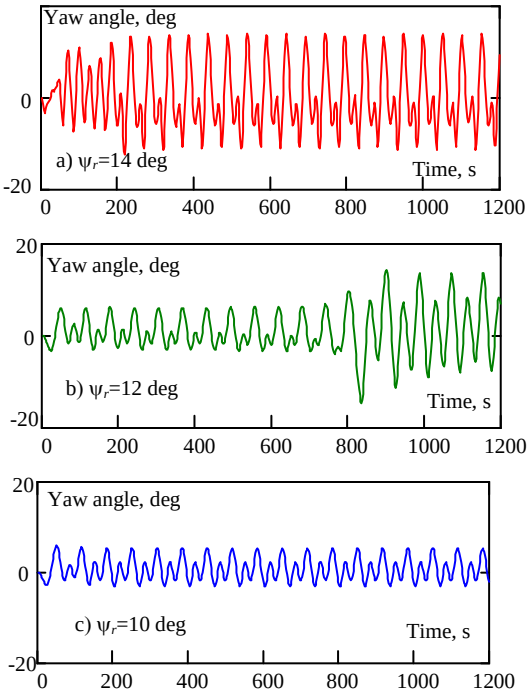

Figure 29 Time histories showing fold bifurcation and subharmonic yaw

The principal mechanisms of broaching are governed by nonlinear dynamics. The continuation method has become one of the most powerful tools to study the behavior of nonlinear systems, and will play a major role in the application of the split time method to surf-riding and broaching. However, continuation techniques were developed for dynamical systems described by a system of ordinary differential equations, and the application of continuation with advanced hydrodynamic codes presents many challenges, mostly caused by hydrodynamic hysteresis (memory effect).

Nevertheless, the first use of continuation method (DERPAR) with a potential flow code (LAMP) has been described by Spyrou et al. (2009). To avoid excessive complexity associated with the memory effect, the diffraction and radiation forces have been approximate with constant added mass and damping coefficient.

As an example of the continuation method, the position of the surf-riding equilibrium for uncontrolled ONR Topsides tumblehome hull in following seas was evaluated, using rudder angle as a control parameter. Figure 30 shows this curve calculated with "conventional" dynamical system described with ordinary differential equations (Spyrou 1996).

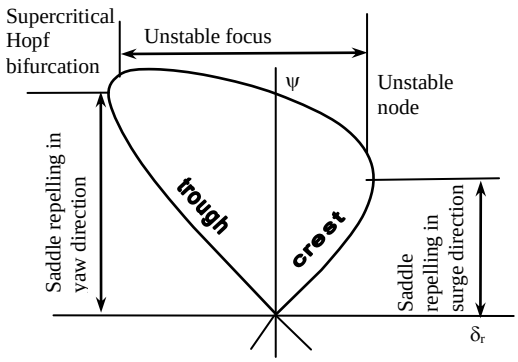

Figure 30 Course angle corresponding to surf-riding equilibria for different rudder angles (Spyrou 1996)

Figure 31 shows the same type of curve calculated using the LAMP implementation of the continuation method. Following the approach described in (Spyrou 1996), the stability of regions of the equilibrium curve was analyzed by examining the eigenvalues. The inset plots the eigenvalues in complex plane for a point on the curve at which the Hopf bifurcation can be expected.

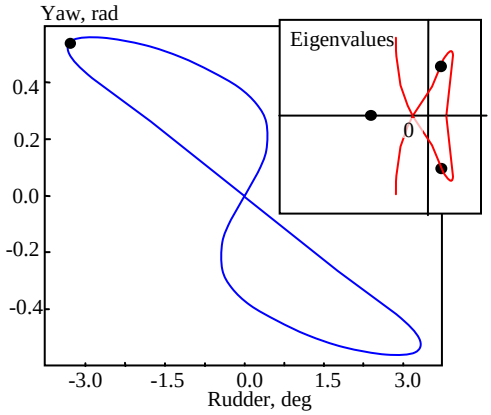

Figure 31 Course angle corresponding to surf-riding equilibria calculation with and DERPAR and LAMP

The eigenvalues are complex with positive real part, which indicates "negative damping" in oscillatory type of motion. This is exactly what could be expected for Hopf bifurcation as surge start to oscillate with increased amplitude until it stabilizes. The numerical simulation at these conditions revealed oscillatory surf-riding, see Figure 32.

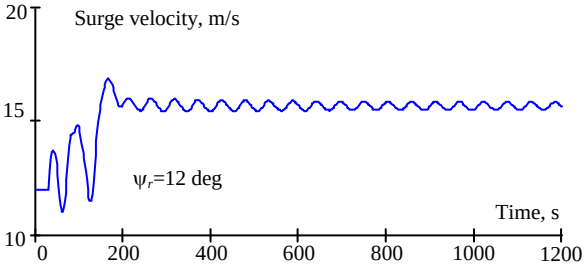

Figure 32 Simulated oscillatory surf-riding – manifestation of Hopf bifurcation.

The ability of an advance potential flow hydrodynamic code to model these non-trivial nonlinear effects may serve as an indication of its qualitative validity. The feasibility of using continuation methods even with a simplified hydrodynamic mode gives a hope that the rich apparatus of Nonlinear Dynamics may be applied for analyzing large-amplitude ship motions simulated these codes.

CONCLUSIONS

The paper considered several aspects related to the extension of the time-split method to the evaluation of the probability of capsizing in stern quartering seas. The main advantage of the time-split method is its ability to use advanced hydrodynamic codes for the evaluation of the probability of extremely rare events. The present work focuses on its application to the problems of pure loss of stability and broaching.

The key aspect of the method's application to pure loss of stability is the consideration of the change of stability in waves. This is done by considering the threshold roll angle corresponding to the maximum of the GZ curve and the critical roll rate leading to capsizing as stochastic processes.

The feasibility of this concept was demonstrated by considering the probability of capsizing of a dynamical system with random piecewise linear stiffness. A special formulation of the random piecewise linear stiffness facilitated a closed form solution. This solution vas verified by a comparison with direct Monte-Carlo simulation and demonstrated convergence.

The application of the time-split method with a code required a method of calculation of instantaneous GZ curve in waves. It was demonstrated that low frequency roll response caused by the Doppler effect may have a significant influence on the rate of upcrossing. As a result, statistical extrapolation may be a method of choice for the non-rare problem: upcrossing through the threshold. The rare problem – the probability of capsizing after upcrossing – may be solved by fitting a joint distribution for the difference between the critical and instantaneous roll rate and the derivative of the distance from current roll angle and the threshold. Statistical extrapolation options also may be considered for rare problem.

The application of the time-split method for surf-riding and broaching first requires a demonstration of the ability of potential flow code to reproduce surf-riding and broaching in regular wave. It has been shown that LAMP is capable to simulate several related phenomena qualitatively correctly. These phenomena include roll and capsizing due to sharp turn, coexistence of surf-riding and surging as well and broaching as a result of fold bifurcation in yaw. It was also shown feasibility of using continuation method with a simplified formulation of LAMP. The results obtained with the continuation method demonstrate it as a useful way to understand physic behind observed phenomena, including oscillatory surf-riding due to Hopf bifurcation. The ability of LAMP reproduce results known from previous theoretical research allows it to be the main hydrodynamic "vehicle" for the implementation of time-split method for broaching.

ACKNOWLEDGEMENTS

The work described in this paper has been funded by the Office of Naval Research under Dr. Patrick Purtell.

Discussions of this work with Prof. Spanos of Rice University and Dr. Art Reed of David Taylor Model Basin were very helpful. The development of the LAMP System has been supported by the U.S. Navy, the U.S. Defense Advanced Research Projects Agency (DARPA), the U.S. Coast Guard, ABS, and SAIC.

REFERENCES

Bassler, C. C., Belenky, V. and M. J. Dipper "Application of Wave Groups to Assess Ship Response in Irregular Seas", Proc. 11th Int. Ship Stability Workshop, Wageningen, the Netherlands 2010.

Belenky, V. L., "A Capsizing Probability Computation Method", J. Ship Research, 1993 Vol. 37, pp. 200- 207.

Belenky, V., Weems, K., M. and W.-M. Lin "Numerical Procedure for Evaluation of Capsizing Probability with Split Time Method", 27th Symposium on Naval Hydrodynamics, Seoul, Korea, 5-10 October 2008.

Belenky, V., and Weems, K.M., "Probabilistic Qualities of Stability Change in Waves," Proc. of 10th Int. Ship Stability Workshop, Taejon, Korea, 2008.

Belenky, V., Reed, A.M. and K. M. Weems "Probability of Capsizing in Beam Seas with Piecewise Linear Stochastic GZ Curve," Proc. of the 10th Int, Conference on Stability of Ships and Ocean Vehicles, St. Petersburg, Russia, 2009.

Campbell, B. and V. Belenky "Statistical Extrapolation for Evaluation of Probability of Large Roll", Proc. of 11th Int. Symp. On Practical Design of Ships and Other Floating Structures, Rio-de-Janeiro, 2010a (Under review)

Campbell, B. and V. Belenky "Assessment of Short-Term Risk with Monte-Carlo Method" Proc. 11th Int. Ship Stability Workshop, Wageningen, the Netherlands 2010b.

Paroka, D., Y. Okura, and N. Umeda (2006), "Analytical Prediction of Capsizing Probability of a

Ship in Beam Wind and Waves", J. Ship Research, Vol. 50, No. 2, pp. 187-195.

Spyrou, K.J. Dynamic instability in quartering seas: The behavior of a ship during broaching, J Ship Research, 1996, Vol. 40, No 1, 46-59.

Spyrou, K. "Dynamic instabilities in quartering seas – part III: nonlinear effects on periodic motions", J Ship Research, 1997, Vol. 41, No 3, pp. 210-223.

Spyrou, K. J., Weems, K. M. and V. Belenky "Verification Of The Patterns Of Surf-riding And Broaching By An Advanced Hydrodynamic Code,", Proc. of the 10th Int. Conference on Stability of Ships and Ocean Vehicles, St. Petersburg, Russia, 2009

Themelis, N., and Spyrou, K.J., "Probabilistic Assessment of Ship Stability," Trans. Soc. of Naval Architects and Marine Engineers (SNAME), vol. 115, 2007.

Weems, K. M., Zhang, S., Lin, W.-M., Shin, Y.-S, and Bennett, J., 'Structural Dynamic Loadings Due to Impact and Whipping.' Proceedings 7th International Symposium on Practical Design of Ships and Mobile Units, The Hague, The Netherlands, 1998.

Yen, T.-G., Zhang, Sh., Weems, K. and W.-M. Lin "Development and Validation of Numerical Simulations for Ship Maneuvering in Calm Water and in Waves" Proc of 28th Symposium on Naval Hydrodynamics (Under review)

APPENDIX 1 DISTRIBUTION OF DERIVATIVE AT UPCROSSING

Consider a random event U in which the stationary differentiable process x upcrossed level a during an infinitesimally small time period following the instant t:

$$U = x(t) < a \cap x(t+dt) > a \qquad \text{(A1.1)}$$

Consider a random event V in which the derivative $\dot{x}(t)$ at an arbitrary instant of time t is positive, but is not larger than a positive value v.

$$V = \dot{x}(t) \le v \cap \dot{x}(t) > 0 \qquad \text{(A1.2)}$$

The probability that upcrossing occurs at an arbitrary instant of time with the derivative not exceeding a positive value v can then be expressed as:

$$P(U \cap V) = P(V \mid U)P(U) \qquad \text{(A1.3)}$$

Here, $P(V|U)$ is the conditional probability that the derivative will not exceed the arbitrary value v if upcrossing occurs:

$$F(v) = P(V \mid U) = \frac{P(V \cap U)}{P(U)} \qquad \text{(A1.4)}$$

The intersection of the events U and V can be presented as a system of inequalities combining (A3.1) and (A1.2).

$$U \cap V = \begin{cases} x(t) < a \\ x(t+dt) > a \\ \dot{x}(t) \le v \end{cases} \Leftrightarrow \begin{cases} x(t) < a \\ x(t) > a - \dot{x}(t)dt \\ \dot{x}(t) \le v \end{cases} \qquad \text{(A1.5)}$$

The probability that the events U and V will intersect can then be expressed as:

$$P(U \cap V) = \int_0^v \int_{a-\dot{x}dt}^{a} f(x) f(\dot{x}) dx d\dot{x} \qquad \text{(A1.6)}$$

Taking into account that the limits of the inner integral differ only by an infinitely small value $\dot{x}dt$,

$$P(U \cap V) = f(a)dt \int_0^v \dot{x} f(\dot{x}) d\dot{x} \qquad \text{(A1.7)}$$

The derivation of the probability of upcrossing at an arbitrary instant of time is trivial, can be found in many sources, and can be done similarly to equation (A1.5) and (A1.7), just without the condition $\dot{x}(t) \le v$.

$$P(U) = f(a)dt \int_0^\infty \dot{x} f(\dot{x}) d\dot{x} \qquad \text{(A1.8)}$$

Finally, the cumulative distribution of the value of the derivative at upcrossing can be expressed as:

$$F(v) = \frac{P(V \cap U)}{P(U)} = \frac{\int_0^v \dot{x} f(\dot{x}) d\dot{x}}{\int_0^\infty \dot{x} f(\dot{x}) d\dot{x}} \qquad \text{(A1.9)}$$

Note that the final distribution does *not* depend on the level a or on the distribution of the process itself. The distribution density can be expressed as:

$$f(v) = \frac{dF(v)}{dv} = \frac{v f(v)}{\int_0^\infty \dot{x} f(\dot{x}) d\dot{x}} \qquad \text{(A1.10)}$$

This is a useful formula for the distribution of the derivative at upcrossing for *any* distribution of the process and its derivative.

APPENDIX 2 DISTRIBUTION OF DEPENDENT PROCESS AT UPCROSSING\

Consider a stationary stochastic process, $x(t)$, that crosses a level a at an arbitrary instant of time t. Consider another stochastic process, $y(t)$, that depends on the process $x(t)$. The objective is to find the probability density distribution of the instantaneous value of the process $y(t)$ when the process $x(t)$ upcrosses the level a.

A random event of upcrossing is defined as:

$$U = \begin{cases} x(t) < a \\ x(t+dt) > a \end{cases}. \qquad \text{(A2.1)}$$

By definition, the cumulative probability distribution is:

$$F_{cr}(y) = P(y \le b \mid U). \qquad \text{(A2.2)}$$

The conditional probability in formula (A2.2) can be expressed as:

$$P(y \le b \mid U) = \frac{P(y \le b \cap U)}{P(U)}. \qquad \text{(A2.3)}$$

Here $P(y \le b \cap U)$ is the probability of occurrence of an upcrossing with the value of the process $y(t)$ not exceeding an arbitrary number b. This random event can be expressed through the following system of inequalities:

$$y \le b \cap U = \begin{cases} x(t) < a \\ x(t+dt) > a \\ y \le b \end{cases} = \begin{cases} x(t) < a \\ x(t) > a - \dot{x}dt \\ y \le b. \end{cases} \qquad \text{(A2.4)}$$

The probability of the random event defined by equation (A2.4) can be expressed trivially through a joint distribution of the process $x(t)$, its derivative and the process $y(t)$:

$$P(y \le b \cap U) = \int_{-\infty}^{b} \int_{0}^{\infty} \int_{a-\dot{x}dt}^{a} f(x, \dot{x}, y) dx d\dot{x} dy. \qquad \text{(A2.5)}$$

The most internal integral in the formula (A2.5) has limits that are infinitely close to each other. Application of the Integral Mean Value Theorem yields:

$$P(y \le b \cap U) = dt \int_{-\infty}^{b} \int_{0}^{\infty} \dot{x} f(a, \dot{x}, y) d\dot{x} dy. \qquad \text{(A2.6)}$$

The probability of upcrossing $P(U)$ can be expressed in similar way:

$$P(U) = dt\, f(a) \int_{0}^{\infty} \dot{x} f(\dot{x}) d\dot{x}. \qquad \text{(A2.7)}$$

The cumulative distribution of the value of y(t) at upcrossing can be expressed by substituting (A2.6) and (A2.7) into (A2.3) and (A2.2):

$$F_c(y) = \frac{\int_{-\infty}^{b} \int_{0}^{\infty} \dot{x} f(a, \dot{x}, y) d\dot{x} dy}{f(a) \int_{0}^{\infty} \dot{x} f(\dot{x}) d\dot{x}} \qquad \text{(A2.8)}$$

The probability density function is obtained from (A2.8) by taking a derivative with respect to y: